Hydrogen Exchange Identifies Native-State Motional Domains Important in Protein Folding†

Key-Sun Kim, James A. Fuchs, and Clare K. Woodward*

Department of Biochemistry, University of Minnesota, St. Paul, Minnesota 55108

Received March 29, 1993; Revised Manuscript Received June 16, 1993®

ABSTRACT: Effects of mutations on hydrogen exchange kinetics, structure, and stability suggest that the slow exchange core is a key element in protein folding. Single amino acid variants of bovine pancreatic trypsin inhibitor (BPTI) have been made with glycine or alanine replacement of residues Tyr 35, Gly 37, Asn 43, and Asn 44. The crystal structures of Y35G and N43G are reported [Housset, D., Kim, K.-S., Fuchs, J., & Woodward, C. (1991) *J. Mol. Biol. 220,* 757–770; Danishefsky, A. T., Housset, D., Kim, K.-S., Tao, F., Fuchs, J., Woodward, C., & Wlodawer, A. (1993) *Protein Sci. 2,* 577–587; Kim, K.-S., Tao, F., Fuchs, J. A., Danishefsky, A. T., Housset, D., Wlodawer, A., & Woodward, C. (1993a) *Protein Sci. 2,* 588–596]. NMR chemical shifts indicate few changes from the wild type (WT) in G37A and N44G. Stabilities of the four mutants were measured by calorimetry and by hydrogen exchange. Values of $\Delta\Delta G_{(WT \rightarrow mut)}$, the difference in ΔG of folding/unfolding between the wild type and mutant, estimated by both methods are in good agreement and are in the range 4.7–6.0 kcal/mol. There is no general correlation between stability and hydrogen exchange rates at pH 3.5 and 30 °C. Exchange occurs by two parallel pathways, one involving small noncooperative fluctuations of the native state, and the other involving cooperative, global unfolding. In the mutant proteins, the rates for exchange by the unfolding mechanism are accelerated by a factor corresponding to the increase in the unfolding/folding equilibrium constant. Rates for exchange by the native-state mechanism either are not affected or are accelerated to varying degrees. NH protons with accelerated exchange rates are primarily in the vicinity of the replacement, which in these mutants corresponds to the flexible loops. The overall effects of destabilizing mutations on hydrogen exchange are similar to those resulting from the addition of 8 M urea (Kim & Woodward, 1993). Motional domains defined by exchange rates are the slow exchange core, flexible loops, and secondary structure not in the core. In BPTI, *the slow exchange core is the folding core*, peptides corresponding to the slow exchange core have native-like structure, and the presence or absence of local structural relaxation around mutation sites reflects the intrinsic local flexibility measured by hydrogen exchange. We propose that this is general for proteins, that the protein segments in the slow exchange core determine the basic fold, and that in compact nonnative states the collapsed region corresponds to the slow exchange core.

Hydrogen exchange rates monitor the internal motions of folded proteins. Exchange with solvent hydrogens of NH that are buried and intramolecularly hydrogen bonded in the crystal structure implies that segments of the protein undergo fluctuations that expose interior sites to water and catalyst (H^+ or OH^-) ions. Isotope exchange rates of protein-bound hydrogens with solvent hydrogens report local packing and flexibility at each of numerous NH sites along the protein backbone. Exchange rate constants for individual hydrogens have been obtained by ^1H NMR for a number of small globular proteins in solution. Hydrogen exchange of buried protons also occurs in protein crystals (Tüchsen et al., 1980; Pedersen et al., 1991; Gallagher et al., 1992). Recent advances in hydrogen exchange applications include identification of compact regions formed early in protein folding (Radford et al., 1992b; Miranker et al., 1991; Udgaonkar & Baldwin, 1988; Roder et al., 1988), structural characterization of compact denatured states (Baum et al., 1989; Pan & Briggs, 1992; Fan et al., 1993; Jeng et al., 1990; Buck et al., 1993; Chyan et al., 1993), and location of specific ligand binding sites (Paterson et al., 1990).

This article reports the effect of single site mutations on the folding thermodynamics and hydrogen exchange kinetics of BPTI. The effects of urea on hydrogen exchange rates in wild type (WT) (Kim & Woodward, 1993) and the effects of mutations on ring flip rates (Kim et al., 1993b) have also been measured. High-resolution crystal structures have been determined for five BPTI mutants from our lab (Housset et al., 1991; Danishefsky et al., 1993).

Protein internal motions assayed by hydrogen exchange are highly variable; some buried regions are highly flexible while others are essentially rigid. The effects of destabilizing mutations on hydrogen exchange rates and protein structure indicate that submolecular motional domains, identified by hydrogen exchange rates, correspond to internal regions that are important to the central logic of protein folding, function, design, and mutational plasticity.

MATERIALS AND METHODS

Construction, expression, and purification of BPTI mutants, described in Housset et al. (1991), are based on procedures of Goldenberg (1988). Protein concentration was measured by absorption at 280 nm using the WT molar extinction coefficient of 5400 (Green & Work, 1953) for WT, G37A, N43G, and N44G. For Y35G, a molar extinction coefficient of 3715 was determined by micro-BCA (Pierce; Smith et al., 1985) and tyrosine titration at pH 13 (Edelhoch, 1967), with the disulfide bonds reduced by sodium borohydride in 10 M urea. Calorimetric experiments and the determination of WT and mutant thermodynamics are described in Kim et al.

† This work is supported by NIH Grant GM26242.

* Author to whom correspondence should be addressed.

® Abstract published in *Advance ACS Abstracts,* September 1, 1993.

0006-2960/93/0432-9600$04.00/0

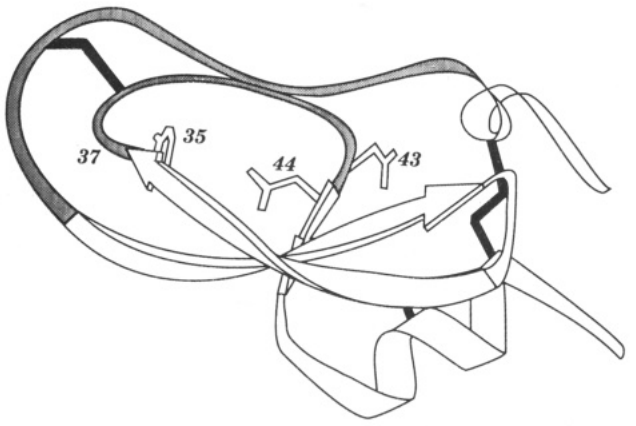

FIGURE 1: Wild-type BPTI. Ribbon representation showing the side chains replaced in mutants Y35G, G37A, N44G, and N43G. Disulfide bonds are solid, and the loops (9–17 and 36–43) are hatched. The drawing was produced with the computer program Adobe Illustrator from the tracing of a figure generated by RIBBONS (Carson, 1987).

(1993a). Values of ΔG(25 °C) for WT and mutants were determined using the denaturational heat capacity change, ΔC_p, of WT measured in the laboratory of Dr. P. Privalov (G. Makhatadze, K.-S. Kim, C. Woodward, and P. Privalov, unpublished results), also described in Kim et al. (1993a).

NMR assignments were made in spectra of 4.5 mM protein (pH 3.5) in 90% H_2O/10% ^2H_2O or 99% ^2H_2O. NOESY spectra with a mixing time of 150 ms were acquired with TPPI (Marion & Wüthrich, 1983). HOHAHA spectra (Davis & Bax, 1985) were taken with TPPI and a mixing time of 45 ms. Water saturation was achieved by a decoupling pulse during the relaxation delay. Spectra were acquired on a General Electric GN Omega-500 spectrometer and processed with FELIX (Hare Research Inc.). Chemical shifts are in ppm from TSP [sodium 2,2,3,3-tetradeuterio-3-(trimethylsilyl)propionate] at 30 °C.

NH and $C_\alpha H$ chemical shifts of G37A, N43G, and N44G are similar to WT; most COSY cross-peak assignments were made tentatively by comparison to WT (Wagner et al., 1987) and confirmed by NOESY and HOHAHA connectivities. For Y35G, cross peaks were assigned by the COSY–NOESY sequential method and confirmed from the spin systems indicated in 3QF-COSY and HOHAHA spectra. Overlapped peaks were assigned from spectra acquired at varying temperatures. In G37A, N43G, and N44G, the cross peak of Cys 14 was not assigned. The Glycine/alanine37 NH was not assigned in proteins other than Y35G because it is shifted upfield to a region of severe spectral overlap (Tüchsen & Woodward, 1987a). Some cross peaks saturated by water decoupling in the H_2O spectrum were recovered from COSY spectra in ^2H_2O and from HOHAHA spectra.

Hydrogen exchange rate constants were determined as described in Kim and Woodward (1993) at pH 3.5, 30 °C, with 4.5 mM protein solutions in 99% ^2H_2O, adjusted with ^2HCl to pH 3.5 (glass electrode reading). For the first 15 min, one-dimensional ^1H NMR spectra were obtained. Magnitude-mode COSY were recorded thereafter with a 33 min data collection time. Hydrogen exchange was followed for 15 days.

RESULTS

Selection and Location of Mutation Sites. BPTI is composed of 58 residues in two long and one very short strand of β-sheet, two helices, two overlapping loops, and three disulfide bonds (Figure 1). The basic BPTI structure has apparently been recruited for a number of important processes in mammals, e.g., blood coagulation (Wun et al., 1988) and Alzheimer's amyloid precursor protein (Kitaguchi et al., 1988; Ponte et al., 1988; Tanzi et al., 1988). The BPTI-related protease inhibitors in these systems retain most of the buried residues of BPTI; differences in protease specificity are due to differences in surface residues, especially those on the overlapping loops (Wenzel & Tschesche, 1984; Kingston & Anderson, 1986; Hynes et al., 1990).

In the mutant proteins, glycine or alanine replaces a residue that, in WT, is involved in unusual buried polar interactions (Figure 1). The buried Asn 43 side chain makes three hydrogen bonds with backbone atoms in the middle β-sheet and N-terminal helix. Each primary amide proton is a donor to a buried backbone oxygen (O7 and O23), and the side oxygen accepts a hydrogen bond from 23 NH [Figure 1 in Tüchsen and Woodward) (1987b)]. Residues 35, 37, and 44 are in an NH–aromatic–NH network; the partially negative center of the Tyr 35 ring interacts with the peptide NH of Gly 37 and with the side-chain NH of Asn 44 [see Figure 10 of Tüchsen and Woodward (1987b)]. Gly 37 NH and Asn 44 HD21 are centered on either side of the ring, packed tightly against the ring and perpendicular to it; this is registered in the ^1H NMR spectrum as a large upfield shift of the resonances for 37 NH and 44 HD21 (Tüchsen & Woodward, 1987b). The stability of the NH–aromatic–NH interaction is not known; preliminary calculations with benzene and ammonia *in vacuo* indicate a value of about 3 kcal/mol for one NH–aromatic interaction (Levitt & Perutz, 1988). Gly 37 is absolutely conserved in known analogs of BPTI and Tyr 35 is conserved in all but two; Asn 44 is occasionally replaced by arginine or lysine.

Buried water molecules in BPTI (Figure 2) are integral parts of its dynamic structure. They hydrogen bond to each other or to buried donors or acceptors [listed in Table II in Tüchsen et al. (1987)]. On average, buried waters are in the location indicated by the crystal structure, but they rapidly exchange with external solvent on a time scale shown to be subsecond by Tüchsen et al. (1987) and in the range 10^{-2}–10^{-8} s by Otting et al. (1991, 1992). The cavity containing waters 111, 112, and 113 is open to solvent when the side chain of Glu 7 is in one of its alternate conformations (Wlodawer et al., 1987). To the extent that the Glu 7 side chain is flexible in solution, this water-containing cavity is open to bulk solvent.

Mutant Structures. Mutant Y35G has extensive rearrangements of the overlapping loops and essentially no changes in the core; it has some of the largest atom displacements reported for a single site mutant (Housset et al., 1991). Loop 36-43 is extensively reordered; buried waters 112, 113, and 122 are not observed, new buried waters are incorporated into the loops, and one end of the β-sheet opens so that the pair of hydrogen bonds between 18 and 35 (O18–N35 and O35–N18) is replaced by new hydrogen bonds. Similarly, since the Tyr 35 ring is missing, its polar interactions with 37 NH and 44 HD21 are replaced by new H-bonds. Consistent with the crystal structure of Y35G, protons with chemical shift differences larger than 0.2 ppm (Figure 3) are located in the loops or in residues 18 and 35. Removal of the tyrosine ring brings the chemical shift of 37 NH (4.34 ppm in WT) into the usual peptide NH spectral region (8.71 ppm). Most chemical shift changes in Y35G are in the direction of random coil chemical shifts, consistent with increased flexibility and exposure of peptide atoms to solvent.

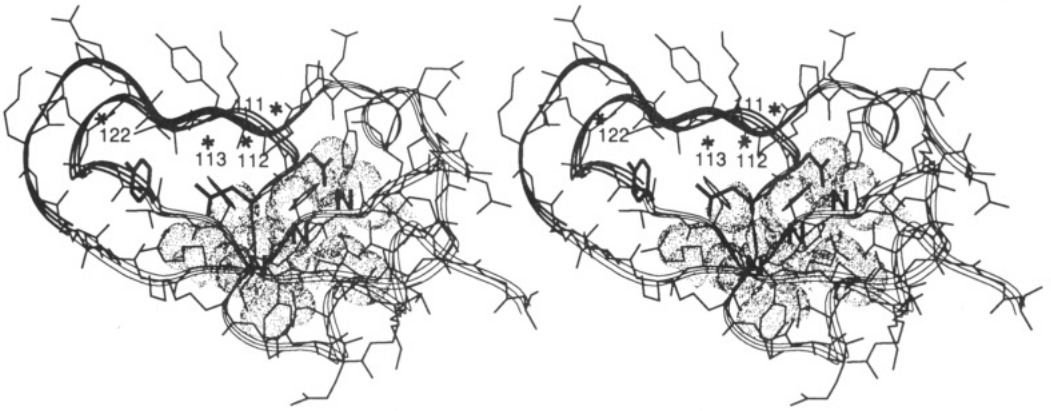

FIGURE 2: Stereo drawing of WT BPTI. The slow exchange core is indicated by dot van der Waals (vdW) surfaces of atoms within 4.5 Å of the NH's of 21–23. The NH's of 21–23 are labeled by a boldface N. The hydrogen exchange defined flexible loops are shown by bold ribbon. Buried waters 111–113 and 122 are represented by stars. The drawing was produced with InsightII for 5PTI.

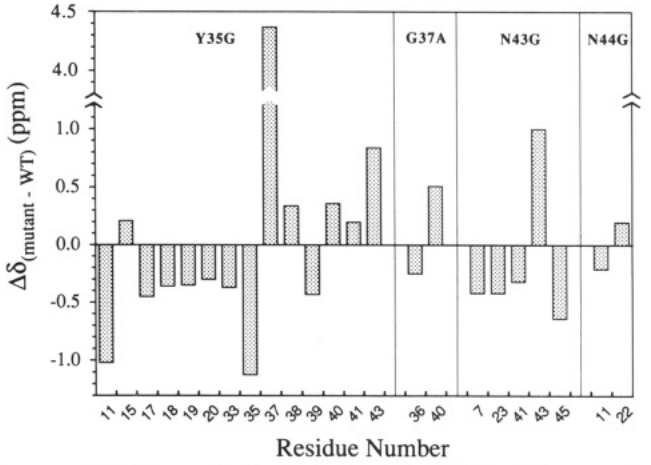

FIGURE 3: Difference in chemical shift (δ) of NH in wild-type and mutant BPTI at 30 °C and pH 3.5. Only NH's with differences >0.2 ppm are shown. A list of NH and $C_\alpha H$ chemical shifts for the mutants is available as supplementary material.

The N43G crystal structure, with the Asn 43 side chain replaced by hydrogen, contains a deep internal crevice containing crystallographic waters and open to solvent (Danishefsky et al., 1993). The molecular surface of N43G is shown in Figure 4. Atoms that are buried donors and acceptors of H-bonds to the Asn 43 side chain in WT make H-bonds to waters in N43G. One of these, the NH of Tyr 23, is among the three slowest exchanging protons; it does not exchange in WT at pH 3.5 unless the protein first unfolds. The exchange behavior of Tyr 23 NH in N43G provides an interesting insight into the mechanism of exchange from the folded state, as discussed below. Since Glu 7 O and Tyr 23 NH each trade an H-bond to the 43 side chain for a protein–water H-bond, their change in chemical shift (Figure 3) is not surprising. The chemical shift changes of 41, 43, and 45 NH suggest a change in the small β-sheet segment composed of residues 44 and 45, consistent with the crystal structure (Danishefsky et al., 1993).

The G37A crystal structure is not solved. The 37 NH–35 ring interaction is the only obvious noncovalent, intramolecular interaction in WT involving Gly 37. The backbone configuration of Gly 37 does not fall in the allowed Φ,ψ space for amino acids with a β-carbon. Our rationale for the construction of mutant G37A was to perturb the polar interaction between 37 NH and Tyr 35. This apparently does occur: In G37A the ring flip rate of Tyr 35 is accelerated by >2 orders of magnitude compared to WT. The chemical shifts of G37A (Figure 3) indicate perturbation in two locations in the loops: Gly 36 NH, adjacent to the mutation site, and Ala 40 NH (the resonance for G37 NH was not assigned).

The N44G crystal structure also is not solved. The ^1H NMR chemical shifts of NH and $C_\alpha H$ fingerprint resonances in WT and N44G are indistinguishable except for 11 and 22, suggesting that any structural changes in the mutant are not widespread. If the only difference between WT and N44G were the loss of the side-chain atoms of Asn 44, N44G would lose the polar interaction with the Tyr 35 ring and one H-bond between a buried water and the other hydrogen on the primary amide side chain. There is another side chain–side chain hydrogen bond (OD1 to Arg 20 HH11) in WT, but this hydrogen bond is not buried.

Effect of Mutations on Hydrogen Isotope Exchange Rates. Hydrogen exchange rate constants of backbone NH protons at 30 °C (pH 3.5) are given in Table I. Rate constants too small to be measured at 30 °C in WT were extrapolated from high temperature, as described in the footnotes to the table. Protons that exchange before 30 min are not listed. These are primarily surface NH that are not intramolecularly H-bonded; their rate constants have been reported (Tüchsen & Woodward, 1985a, 1987a; Tüchsen et al., 1987). Hydrogen exchange from native proteins may occur by either of two pathways: one an unfolding mechanism in which exchange is from a denatured state, and the other a mechanism for exchange from the folded state (Woodward et al., 1982; Kim & Woodward, 1993). The introduction of destabilizing mutations or chemicals affects exchange by each pathway differently, as discussed in Kim and Woodward (1993). Comparisons of WT and mutant exchange rates are shown in Figures 5 and 6.

In Figure 5, each data point represents one NH plotted to show its exchange rate in G37A or N44G on the y-axis and its exchange rate in WT on the x-axis. For an NH with the same exchange rate in mutant and WT, the data point is on the diagonal. Destabilizing mutations affect exchange rates in one of three ways. First, the mutation accelerates the rates of protons exchanging by the unfolding mechanism [see Kim and Woodward (1993) for further discussion]. The eight slowest protons exchange by unfolding in G37A or N44G; all have similar exchange rate constants, approximated by the dotted line in Figure 5. Among the protons in this group are the very slowest exchanging in WT, namely, 21, 22, and 23, which in WT also exchange by the unfolding mechanism; these can be used to estimate $\Delta\Delta G_{(WT \rightarrow mut)}$ (below). The other five NH's along the dotted line are those that exchange by the unfolding mechanism in the mutant but not in WT; these are located along the middle strand of β-sheet in the

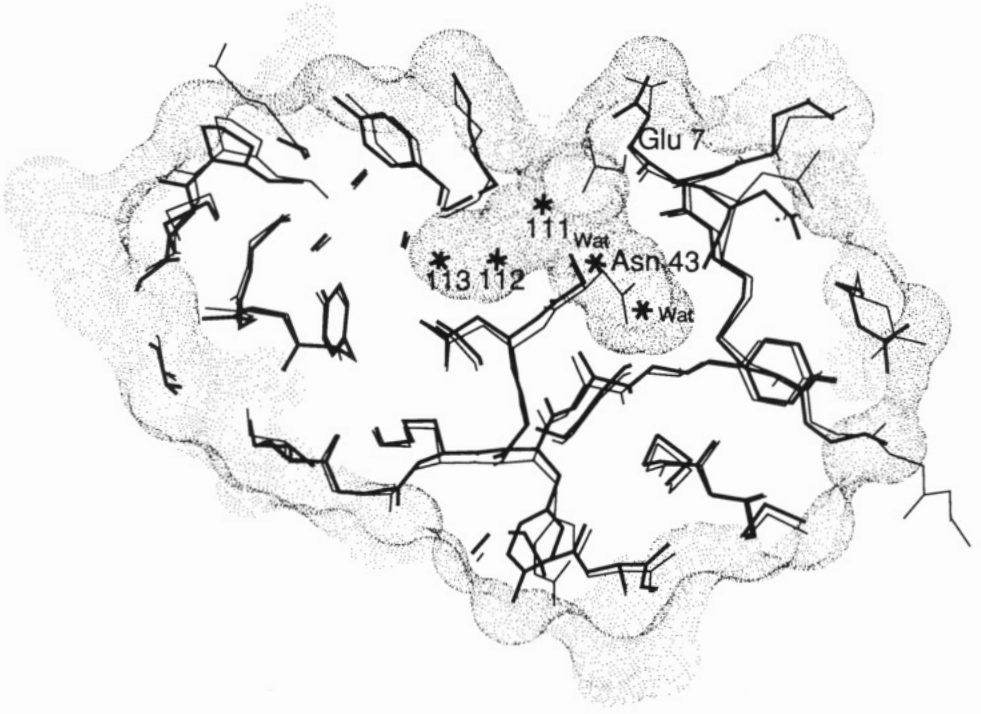

FIGURE 4: Cross-section of the crystal structure of mutant N43G molecular surface (Danishefsky et al., 1993). Dots represent the molecular surface (Connolly, 1983). The cavity (left) contains waters 111–113 in both WT and mutant. The crevice (right) created in N43G by removal of the Asn 43 side chain contains two waters (labeled Wat). Stick models of WT (thin lines) and N43G (bold lines) are overlaid. The Glu 7 side chain (top) has two positions in WT, one of which opens waters 111–113 to bulk solvent; in solution, the Glu 7 side chain presumably samples both conformations (see text for discussion). In N43G, the Glu 7 side chain is in the conformation that opens the left cavity as well as the right crevice.

core of BPTI. Second, a number of protons show no detectable effect on exchange rates from destabilizing mutations; they have the same rate constant in WT and in mutant. These are more rapidly exchanging buried protons; their data points lie close to the diagonal of Figure 5. They exchange by the native-state mechanism in both WT and mutant. Third, mutations accelerate the rates of some protons exchanging from the folding state. These are the protons represented by points which lie above the dotted line and to the left of the diagonal in Figure 5; their residue numbers are indicated. Their locations in the three-dimensional structure tend to be either at the open end of the two strands of twisted β-sheet hairpin (residues 18 and 35), in the small strand of β-sheet (residues 44 and 45), or in the overlapping loops (residues 10, 16, 41, 36).

Figure 6 shows similar behavior for mutants Y35G and N43G, which are more destabilized than G37A and N44G. The dotted line marking protons that exchange by the unfolding mechanism in the mutant is higher than in Figure 5, reflecting the greater destabilization of these mutants. A few protons lie along the diagonal; their exchange rates are not affected by the mutation. Many protons lie above the dotted line and to the left of the diagonal; their exchange from the folded state is accelerated in the mutant. There are more protons in this category than in mutants G37A and N44G (Figure 5), but like G37A and N44G the most perturbed protons are in the flexible loops. In Y35G, residues 18 and 35 exchange too fast to be observed (circles at the top of Figure 6), consistent with the Y35G crystal structure in which the WT hydrogen bonds between 18 and 35 are replaced by water–protein hydrogen bonds (Housset et al., 1991). In N43G, 44 NH is too fast to observe and 18, 35, and 45 are accelerated, indicating perturbation of the small β-sheet (44 and 45) and the open end of the central β-sheet (18 and 35). In addition to 18, 35, 44, and 45, the largest effects are observed for loop protons (residues 10, 16, 19, 34, and 36). In Y35G, the loop rearrangements increase loop flexibility and hydrogen exchange rates of loop protons (10, 16, 19, 34, 36).

In summary, destabilizing mutations increase exchange rates for the unfolding mechanism. For the native-state mechanism, destabilizing mutations do not affect the exchange rates of many NH's, but do accelerate the exchange of some in the vicinity of the substitution. Three of the mutations are in the flexible loops (Y35G, G37A, and N44G), and this explains the increased exchange rates in the flexible loops and at the open end of the β-sheet hairpin turn. In N43G, however, the mutation is not in the loops. The crystal structure of N43G indicates perturbation of the small 44,45 β-sheet, as well as creation of a very large crevice near the core region (Figure 4), and this can explain the acceleration of 44 and 45 in N43G. The acceleration of 18 and 35 in N43G is intriguing in view of our previous observation that crystallization of BPTI markedly decreases the exchange of 18 and 35 (Gallagher et al., 1992), suggesting that the open end of the sheet serves as a flexible connection between the rigid core and the flexible loops.

Folding Thermodynamics of BPTI and Mutants. The mutants are highly destabilized compared to WT; the folding midpoint temperature, T_m, is decreased by 15–30 °C (Table II). The values of $\Delta\Delta G°_{(WT\rightarrow mut)}$ are exceptionally large for a single amino acid replacement. Thermodynamic parameters in Table II are determined by differential scanning calorimetry as described in Kim et al. (1993a). Hydrogen exchange rates may also be used to estimate $\Delta\Delta G°_{(WT\rightarrow mut)}$ (Kim & Woodward, 1993). The values of $\Delta\Delta G_{(WT\rightarrow mut)}$ determined by the two methods (Table II) are in good agreement, given the experimental uncertainties. Differences between calorimetric and hydrogen exchange values may arise from a number of factors. Calorimetry was performed at pH 2 to minimize titration effects and hydrolysis of the protein (Kim et al.,

Table I: Hydrogen Exchange Rates (min^{-1}) of BPTI and Variants at 30 °C and pH 3.5

no.	WT	Y35G	G37A	N43G	N44G
5	3.8×10^{-4}	2.4×10^{-3}	5.3×10^{-4}	8.8×10^{-3}	1.6×10^{-3}
6	2.2×10^{-4}	5.4×10^{-4}	1.2×10^{-4}	2.0×10^{-3}	3.0×10^{-4}
7	1.2×10^{-4}	4.2×10^{-4}	1.5×10^{-4}	1.5×10^{-3}	3.2×10^{-4}
10	4.7×10^{-4}		1.4×10^{-2}	9.0×10^{-3}	2.3×10^{-3}
11				1.8×10^{-2}	
14	3.3×10^{-3}				
16	5.8×10^{-4}			3.9×10^{-3}	2.9×10^{-3}
18	5×10^{-7} [a]		5.1×10^{-4}	2.3×10^{-4}	5.8×10^{-4}
19	4.6×10^{-3}		3.0×10^{-3}	6.6×10^{-3}	7.6×10^{-3}
20	9×10^{-8} [a]	6.7×10^{-5}	1.3×10^{-5}	1.0×10^{-4}	1.3×10^{-5}
21	2×10^{-9} [b]	2.9×10^{-5}	6.3×10^{-6}	4.5×10^{-5}	4.9×10^{-6}
22	2×10^{-9} [b]	2.7×10^{-5}	6.8×10^{-6}	5.1×10^{-5}	6.7×10^{-6}
23	2×10^{-9} [b]	4.3×10^{-5}	5.6×10^{-6}	8.5×10^{-5}	9.6×10^{-6}
24	7×10^{-7} [a]	1.4×10^{-4}	1.4×10^{-5}	1.5×10^{-4}	1.1×10^{-5}
27	1.2×10^{-3}	7.0×10^{-3}	3.2×10^{-3}	3.8×10^{-3}	5.1×10^{-3}
28	4.1×10^{-4}	4.1×10^{-3}	3.0×10^{-4}	4.6×10^{-4}	7.6×10^{-4}
29	3×10^{-6} [a]	5.9×10^{-5}	1.4×10^{-5}	1.1×10^{-4}	1.1×10^{-5}
30			1.1×10^{-2}	1.3×10^{-2}	2.0×10^{-2}
31	5×10^{-7} [a]	5.5×10^{-5}	7.8×10^{-6}	7.8×10^{-5}	1.1×10^{-5}
32	1.9×10^{-3}	4.1×10^{-3}	1.6×10^{-3}	1.5×10^{-3}	4.8×10^{-3}
33	6×10^{-7} [a]	9.3×10^{-5}	1.1×10^{-5}	5.3×10^{-5}	1.6×10^{-5}
34	2.3×10^{-3}		6.2×10^{-3}	3.8×10^{-3}	3.9×10^{-3}
35	2×10^{-6} [a]		2.6×10^{-3}	1.2×10^{-3}	4.2×10^{-4}
36	7.7×10^{-5}	4.7×10^{-2}	4.6×10^{-3}	4.7×10^{-3}	2.8×10^{-3}
38		1.4×10^{-3}			1.0×10^{-2}
40			1.1×10^{-2}		
41	4.0×10^{-4}				1.9×10^{-2}
44	2×10^{-6} [a]	3.6×10^{-3}	5.0×10^{-4}		1.2×10^{-3}
45	6×10^{-7} [a]	5.6×10^{-4}	4.6×10^{-5}	8.2×10^{-4}	7.0×10^{-5}
47					1.6×10^{-2}
51	5.1×10^{-5}	3.0×10^{-4}	5.4×10^{-5}	3.8×10^{-4}	4.4×10^{-5}
52	2.6×10^{-5}	1.0×10^{-4}	2.9×10^{-5}	8.4×10^{-5}	6.8×10^{-5}
53	4.6×10^{-5}	1.2×10^{-4}	3.3×10^{-5}	1.3×10^{-4}	5.9×10^{-5}
54	2.4×10^{-4}	2.7×10^{-4}	1.9×10^{-4}	3.9×10^{-4}	2.4×10^{-4}
55	1.8×10^{-5}	1.8×10^{-4}	3.6×10^{-5}	2.8×10^{-4}	3.6×10^{-5}
56	8.0×10^{-4}	1.5×10^{-3}	7.3×10^{-4}	1.8×10^{-3}	5.9×10^{-4}

[a] WT rate constants were estimated by extrapolation to 30 °C from the average of rate constants at 36 °C measured by Wagner (1983) and by F. Tao (unpublished results), using an activation energy of 35 kcal/mol. [b] WT rate constants were estimated by extrapolation of high-temperature rate constants using an activation energy of 78 kcal/mol. This activation energy, at pH 3.5 and with no added salt, was obtained for 21–23 over the interval 45–72 °C from rate constants at 10 temperatures measured by K.-S. Kim and F. Tao (unpublished results) and the 45 °C rate constant reported by Richarz et al. (1979).

1993a), while the hydrogen exchange experiments were carried out at pH 3.5 where exchange is in the base-catalyzed regime; at pH 2, most protons exchange by the acid-catalyzed mechanism. In this pH range, the N- and C-terminal salt bridge is broken due to protonation of the C-terminal carboxyl (Brown et al., 1978; Tüchsen & Woodward, 1985a). The main source of uncertainty in the calorimetric free energy changes (Table II) is the values of ΔC_p, which are not rigorously determined for the mutants [see Kim et al. (1993a)]. In the hydrogen exchange estimate of $\Delta\Delta G°$, the main source of uncertainty is the extrapolation from high temperature to 30 °C values of k_{obs} for 21, 22, and 23, as described in Table I.

Y35G has a larger change in ΔH compared to other mutants with similar $\Delta G°$ values (Table II), indicating a significant loss in Y35G of enthalpic interactions such as H-bonding and other polar interactions. This is consistent with the loss of the NH–aromatic–NH interactions of 37 and 44 with the Tyr 35 ring described above and replacement of two intramolecular H-bonds of the β-sheet (18 and 35) for protein–water H-bonds (Housset et al., 1991). There is a compensatory decrease in ΔS, since ΔG(25 °C) values are about the same as in other mutants, which suggests an increased flexibility of the folded

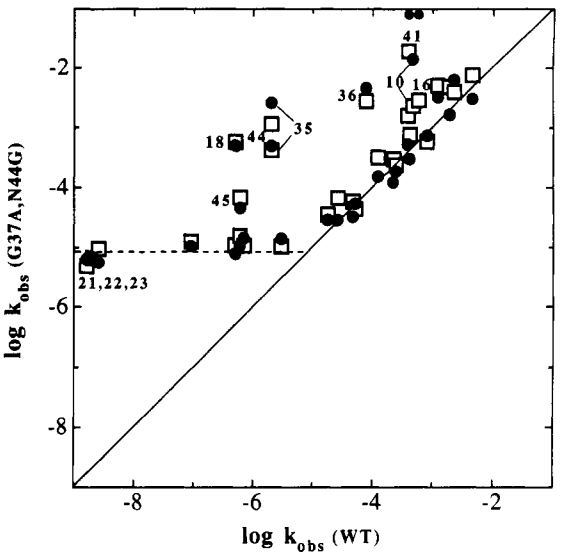

FIGURE 5: Comparison of hydrogen exchange rate constants (min^{-1}) of wild-type BPTI to G37A and N44G. Symbols show the rate constants of one NH proton in G37A (●) or N44G (□) in the mutant (y-axis) and in WT (x-axis). If exchange rate constants of the proton are the same in WT and mutant, the symbol falls along the diagonal. Along the top of the figure, small symbols represent NH's of 41 and 16 in G37A, which exchange too rapidly to measure in these experiments.

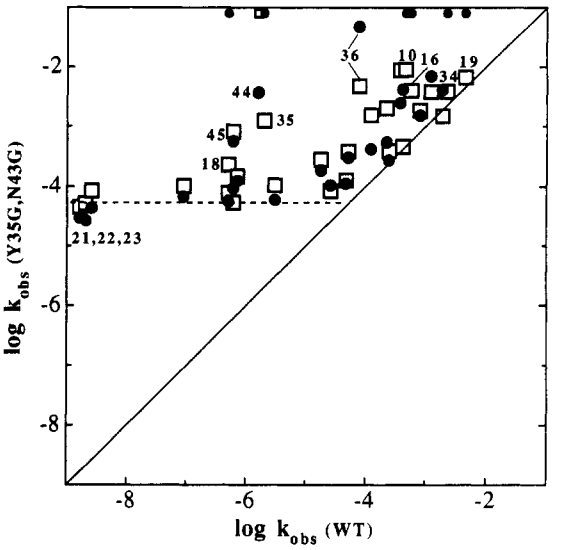

FIGURE 6: Comparison of hydrogen exchange rate constants (min^{-1}) of wild-type BPTI to Y35G and N43G. Symbols show the rate constants of one NH proton in Y35G (●) or N43G (□) in the mutant (y-axis) and in WT (x-axis), as in Figure 4. Along the top of the figure, small symbols represent NH's of 18, 35, 10, 16, 34, and 19 in Y35G and 44 in N43G, which exchange too rapidly to measure in these experiments.

state, most likely from the increased mobility of overlapping loops 11–18 and 34–44. This is consistent with the increase in Y35G of hydrogen exchange rates in this region and of ring flip rates for Tyr 23 and Phe 45 (Kim et al., 1993b).

Substitution of Gly 37 by alanine decreases $\Delta G°$ by ~5 kcal/mol, even though in WT crystal structure its only apparent interaction is with the Tyr 35 ring. The ring flip rate of Tyr 35 is slow in WT but becomes very fast in G37A, indicating a disruption of the ring–NH polar interactions (Kim et al., 1993b). Other parts of the protein are similar to WT in hydrogen exchange and aromatic ring flip rates. Some of the destabilization of G37A may arise from an energetically unfavorable torsion angle.

Table II: Thermodynamic Parameters of BPTI and Its Variants

	T_m (°C)[a]	$\Delta H(T_m)$ (kcal/mol)[a]	ΔG(25 °C) (kcal/mol)[a]	$\Delta\Delta G$(cal) (kcal/mol)[a]	$\Delta\Delta G$(HX) (kcal/mol)[b]
WT	87	70	9.0		
Y35G	69	38	4.0	5.0	5.7
G37A	66	47	4.1	4.9	4.7
N43G	55	46	3.3	5.7	6.0
N44G	66	49	4.3	4.7	4.7

[a] Obtained by differential scanning calorimetry at pH 2.0, as described in Materials and Methods and in Kim et al. (1993a). Values for WT, Y35G, and N43G were reported in Kim et al. (1993a). Standard deviation for curve fitting and experimental error is approximately 0.5 °C, 1.0 kcal/mol, and <0.7 kcal/mol for T_m, $\Delta H(T_m)$, and ΔG(25 °C), respectively. [b] The change in ΔG between WT and BPTI variants from hydrogen exchange rate constants of 21–23 at pH 3.5, 30 °C (Kim & Woodward, 1993).

DISCUSSION

A number of studies have correlated changes in protein tertiary structure and folding energetics arising from site-directed substitutions at one or several sites. We have expanded this approach by determining, in addition, the changes in a third property, local flexibility. Hydrogen exchange rates, aromatic ring flip rates, and folding thermodynamics have been measured for BPTI mutants with alanine or glycine replacements at positions 21–23, 35, 37, and 43–45. The crystal structures of five of these mutants are determined (Housset et al., 1991; Danishefsky et al., 1993). Here we report the hydrogen exchange and thermodynamic results for mutations at 35, 37, 43, and 44; ring flip rates are presented elsewhere (Kim et al., 1993b). Similar results have been obtained for the other four mutants (F. Tao, J. Fuchs, and C. Woodward, unpublished results). For wild-type BPTI, we have determined the hydrogen exchange rates of buried NH in 8 M urea solutions (Kim & Woodward, 1993) and in crystals (Gallagher et al., 1992), of buried NH hydrogen bonded to buried waters (Tüchsen et al., 1987), of asparagine primary amide protons that are buried and intramolecularly H-bonded (Tüchsen & Woodward, 1987b,c), and of protons on the protein surface hydrogen bonded to solvent water (Tüchsen & Woodward, 1985a,b, 1987a). Considered together, the correlations of local flexibility with structure and stability lead to a number of generalizations and testable hypotheses relating protein dynamics, structure, and folding.

Hydrogen Exchange Identifies Submolecular Motional Domains. One of the most salient features of hydrogen exchange is the vast range of exchange rates in one protein. Protons that are buried and intramolecularly hydrogen bonded in the crystal structure have rates that vary over >8 orders of magnitude. The spread of rate constants actually observed depends on the folding/unfolding equilibrium constant (Kim & Woodward, 1993). The large differences in local flexibility among submolecular regions reflected by hydrogen exchange are not apparent in the published results of other experimental or theoretical methods.

From the distribution of exchange rate constants of interior protons, we distinguish three domains of varying internal mobility. (i) The slow exchange core region contains a small cluster of the slowest exchanging hydrogens. It is the most rigid interior region; local motions seldom if ever lead to the transient unpacking necessary to support hydrogen exchange. (ii) The most flexible buried region(s) exchanges rapidly (though not as rapidly as surface protons) and often is made up of loops. (iii) Secondary structural regions, not in the core, contain protons with exchange rates intermediate between i and ii. A fourth category, surface NH, is for the most part more rapidly exchanging than interior protons, but these exchange rates can be several orders of magnitude slower than those of extended oligopeptides (Tüchsen & Woodward, 1985a). The implications of slow exchange of surface protons have been discussed (Tüchsen & Woodward, 1985b).

The slow exchange core is the region containing the 3–8 slowest exchanging protons and the atoms packing them. Large proteins with more than one cooperative folding unit are expected to have more than one slow exchange core. Core protons are in segments of secondary structure that are packed by hydrophobic side chains, especially aromatics. Secondary structural elements containing core hydrogens usually are not contiguous.

Figure 2 shows hydrogen exchange defined regions of BPTI. The slow exchange core corresponds to the central β-sheet NH of 21–23 and surrounding atoms (Hilton et al., 1981). Dot surfaces of heavy atoms within 4.5 Å of 21–23 NH are shown in Figure 2; these are side-chain atoms of 20–23, 30, 33, 43, 45, and 51 and backbone atoms of residues 20–24, 30–33, and 45 (Kim et al., 1993a). The core atoms are all on the three β-sheet segments, except for the side chain of residue 51 in the C-terminal helix. The BPTI core contains the lowest *B* factors and the most highly conserved hydrophobic groups, consistent with the Lumry knot hypothesis (below). The hydrophobic groups are aromatic rings, except for buried side-chain atoms of cystine 30–51.

The most flexible buried regions in BPTI, by hydrogen exchange criteria, are the overlapping loops shown in boldface in Figure 2. The loops (9–17 and 36–43) enclose the Tyr 35 ring packed by polar groups and buried water molecules. The flexible loops of BPTI contain the protease binding site around Lys 15. We expect that hydrogen exchange defined flexible regions in other proteins will tend to be loops in which structure is dominated by polar interactions with geometric constraints that result in less dense packing. Protons with intermediate exchange rates are at the open end of the β-sheet and in the N- and C-terminal helices (not highlighted in Figure 2).

The Slow Exchange Core Is the Protein Folding Core. Comparison of the slow exchange core with the protein region first protected from exchange during folding reveals an important correlation: the slow exchange core is the folding core. In three proteins, for which both out-exchange and protection data are published, *the last hydrogens out mark the region where hydrogens are first protected.* Or, the protons exchanging last from the native protein are among the first slowed when the protein folds. The best developed case is lysozyme. The five slowest exchanging protons are located in three helices within the α-domain containing five helices (Radford et al., 1992a). The first NH sites to be protected include these and other protons in the α-domain, plus four other protons not in the α-domain (Miranker et al., 1991; Radford et al., 1992b). The latter are apparently slowed even in thermally denatured lysozyme (Mirankder et al., 1991). In BPTI, 21–23 are among the first peptide NH's protected in refolding experiments (Roder & Wüthrich, 1986). In cytochrome *c*, the N- and C-terminal helices contain the slowest exchanging NH's (Jeng et al., 1990), which are among the first protected NH's during folding (Roder et al., 1988).

For proteins in which the slow exchange core is the folding core, we expect that the collapsed region in compact denatured state(s) corresponds to the slow exchange core in the native state, while the disordered regions correspond to hydrogen exchange categories ii and iii above. This suggestion is consistent with data on alcohol-denatured proteins (Pan & Briggs, 1992; Fan et al., 1993), lysozyme in trifluoroethanol

(Buck et al., 1993), the molten globule of α-lactalbumin (Chyan et al., 1993), and cytochrome *c* at low pH (Jeng et al., 1990).

An intriguing possibility emerges: that the folding regimen roughly corresponds to regions of the native protein ranked in reverse order of their exchange rates, i.e., that folding proceeds in these stages: collapse of the slow exchange core, followed by packing of the secondary structure elements not in the core, and then packing of the flexible loops. At each stage, the partially folded intermediates are expected to be formed by multiple pathways. It has been demonstrated that the initial collapse of the core occurs by multiple parallel pathways (Radford et al., 1992b; Pain, 1992).

This offers a simplified method for identification of the folding core since the last protons out are usually easier to determine than the first ones protected. The last 3–8 protons to exchange from a protein can be identified at any convenient temperature or pH, since the order in which labile protons exchange from a protein is independent of temperature and pH (at pH > 3), as shown in bulk tritium–hydrogen exchange experiments (Woodward & Rosenberg, 1971). The rank order of exchange does not change with pH since the pH dependence of exchange resides in the chemical step, which is the same for all protons [see Kim and Woodward (1993)]. The rank order of exchange is temperature independent because there is an inverse correlation between the magnitude of k_{obs} and its apparent activation energy; smaller exchange rate constants have larger activation energies (F. Tao, unpublished results). Thus, in a relatively simple experiment one can determine the core. Identification of the slow exchange core does not provide the rich detail of the elegant experiments reported by Radford et al. (1992b) and Chyan et al. (1993), but it does point to the key submolecular domain of the protein.

For prediction of protein folded structure from the primary sequence, knowledge of the slow exchange core could be helpful as an indicator of long-range tertiary interactions important both in the first stages of folding and in the native structure. The possibility that the rigid, hydrophobic core consists of the segments that are compact early in protein folding is consistent with the hydrophobic zipper model of Dill et al. (1993). The potential usefulness of the slow exchange core in protein structure prediction and its relative ease of measurement make an argument for its inclusion in protein databases.

Mutation Site Rearrangements and Hydrogen Exchange Measure the Same Property: Local Flexibility. The relaxation of local structure in response to substitution of a larger side chain by a smaller one depends on whether the substitution is in a region that is inherently flexible or rigid in the WT protein. The local flexibility assayed by structural rearrangements associated with amino acid replacement is, we propose, the same property monitored by hydrogen exchange. In BPTI, there is a strong correlation between mutational plasticity and hydrogen exchange rates. The flexible (rapidly exchanging) loops in BPTI undergo significant rearrangements when loop residues are replaced, as illustrated by the crystal structure of Y35G (Housset et al., 1991) and by the accelerated ring flip rate of Tyr 35 in G37A (Kim et al., 1993b). In contrast, few or no rearrangements are observed when replacements are in the slow exchange core of BPTI (Kim et al., 1993a).

When side-chain replacements are made in the more rigid regions of a protein, effects on stability should be additive [cf. Wells (1990)]. However, replacements of amino acids in flexible regions may not be additive, even if they are at nonoverlapping sites in the native structure.

Rational Design of Ligand Binding Sites Is Favored in the Slow Exchange Core. The tendency of the slow exchange core not to relax around mutation sites suggests the core as a region favorable for laboratory design of ligand binding sites. This is because the predictability of ligand binding behavior should be higher when there are fewer rearrangements arising from the designed replacement or removal of atoms.

Naturally occurring specific binding sites, evolved after random trial and error on the millennial time scale, tend not to be in the slow exchange core but rather in mobile loops. Polar packing interactions, with their attendant specific geometry and segmental flexibility, make loop regions more tractable for juxtaposition of reactive groups and more versatile for regulatory conformational rearrangements.

Fragments Corresponding to the Slow Exchange Core Will Give Native-like Structure. Fragments of a protein corresponding to the slow exchange core should acquire the same fold that they do in the parent molecule (provided the fragment is not so unstable that unfolding is favored under the experimental conditions). While interactions in flexible regions contribute significantly to the magnitude (or sign) of ΔG for folding/unfolding, we expect that the slow exchange core region governs the supersecondary architecture and the basic folding pattern. In BPTI, the fragment corresponding to the slow exchange core has been constructed, albeit with a different model in mind, and it has the same basic fold as native BPTI (Oas & Kim, 1988). We predict the same for other proteins and suggest that protein design may usefully begin with sequences (or hydrophobic patterns) corresponding to the slow exchange core, followed by later additions of other structural elements.

Slow Hydrogen Exchange Is Not Due Simply to Intramolecular H-Bond Formation. The structural reasons for slow exchange in proteins, in protein fragments, and in compact denatured proteins are of great interest. It is, no doubt, often the case that slowly exchanging protons are in intramolecular H-bonds, but this cannot be presumed for every instance of slow exchange. In proteins, all NH's are H-bonded either intramolecularly or intermolecularly to waters; the presence of an H-bond *per se* does not explain the large distribution of exchange rate constants. Cases of fast exchange are observed for intramolecularly H-bonded NH's, while a number of protons in water–protein H-bonds have slow exchange. The retardation of exchange is a function of the (dynamic) accessibility of catalyst and water to the exchanging NH and a function of the reactivity of the NH with catalyst to form a charged intermediate. In very rigid regions of the protein, although catalyst and water may be within interaction distance, local rigidity may constrain the NH in an unfavorable geometry that restricts reactivity.

Surface protons of BPTI, H-bonded to surface waters in the crystal structure, exchange significantly slower than oligopeptide protons (Tüchsen & Woodward, 1985). Another instructive instance of very slow exchange of a proton H-bonded to water is Tyr 23 NH in the mutant N43G. In wild-type BPTI, 23 NH is in the slow exchange core. In N43G, 23 NH lines a deep crevice and is hydrogen bonded to a crystallographic water (Figure 4). The crevice is open to the molecular surface, and it is safe to assume that the water hydrogen bonded to 23 NH exchanges with bulk waters on a subsecond time scale. Nevertheless, N43G exchanges so slowly from the folded state that we observe its exchange at pH 3.5 only when the protein unfolds. This is in contrast to NH protons that are H-bonded to naturally occurring, buried waters in the flexible loops of WT; these exchange almost as rapidly as surface

protons and with the expected first-order dependence on catalyst ions, meaning that they are exposed, in the dynamical sense, to catalyst as well as solvent (Tüchsen et al., 1987). We attribute the slow exchange of Tyr 23 NH in N43G to the rigidity of the protein core, which may prevent access of catalyst ion to the crevice surface and/or restrict the NH in a geometry unfavorable to proton extraction by catalyst.

Estimates of $\Delta\Delta G_{(WT\rightarrow mut)}$ from Hydrogen Exchange Data. When a proton exchanges by the unfolding mechanism in both WT and mutant, $\Delta\Delta G_{(WT\rightarrow mut)}$ can be estimated from the ratio of its observed rate constant in WT to its observed rate constant in the mutant (Tao et al., 1993; Kim & Woodward, 1993). Comparisons of $\Delta\Delta G_{(WT\rightarrow mut)}$ values measured by hydrogen exchange and by calorimetry are given in Table II. The reasonable agreement of $\Delta\Delta G_{(WT\rightarrow mut)}$ measured by the two methods supports use of the hydrogen exchange method for estimation of $\Delta\Delta G_{(WT\rightarrow mut)}$ and the validity of the two-process model (Kim & Woodward, 1993).

Motions That Expose Buried Protons for Exchange Are Highly Localized. Internal motions of proteins that underlie the folded-state exchange mechanism are not known with certainty. Two models have been offered. In the non-cooperative fluctuations (or penetration) model, small, non-cooperative motions on the order of tenths of angstroms occasionally permit transient access of buried, H-bonded NH to water *and* catalyst, and exchange is from a conformation very similar to the crystal structure (Woodward & Hilton, 1980; Woodward et al., 1982). Specific mechanisms suggested for non-cooperative fluctuations leading to hydrogen exchange are "mobile defects" in protein packing (Lumry & Rosenberg, 1975) and transient formation of channels from bulk solvent to interior sites (Richards, 1979). In the local unfolding model, segments of secondary structure undergo cooperative hydrogen bond breaking, which brings buried sites into contact with solvent (Englander, 1975; Englander & Englander, 1978). The pros and cons of these two models have been reviewed [Woodward et al. (1982) and references therein, Hilton et al. (1981) and Englander and Kallenbach (1984)].

In the non-cooperative fluctuations (or penetration) model, the chemical exchange step occurs from a conformation in which atom positions are approximated by the crystal structure (Woodward et al., 1982). This model predicts that neighboring protons will often have very different rates and activation energies for exchange, i.e., exchange is highly localized. Several results indicate this behavior. Exchange of two protons bound to the same atom, the primary amide nitrogen of Asn 43 or Asn 44, is not correlated even though rotation about the amide C–N bond is rapid on the exchange time scale (Tüchsen & Woodward, 1987c). In lysozyme (Radford et al., 1992; Pedersen et al., 1993) and in leucine zipper peptides (Goodman & Kim, 1991), there are helices in which exchange rates are more rapid on the solvent side of the helix and slower on the packed side. This implies that the amphoteric helix is intact and packed when exchange occurs, and this is consistent with a non-cooperative fluctuations model. Also in lysozyme, other nonhelical, but adjacent, NH's have very different exchange rates (Pedersen et al., 1993), again consistent with a penetration model. Last, although our BPTI mutants induce massive destabilization of the molecule, many protons have exchange rates that are not perturbed relative to wild type, as is discussed next.

There Is Not a General Correlation between Global Stability and Exchange from the Folded State. These single site mutants are very highly destabilized (Table II). As expected, the higher the value of $\Delta\Delta G_{(WT\rightarrow mut)}$, the greater the rate of exchange by the unfolding mechanism. However, for exchange by the native-state mechanism (the more rapidly exchanging protons), there is no general correlation with stability. For native-state exchange, in the less destabilized mutants, G37A and N44G, either there is no effect or rates are increased for NH in the vicinity of the mutation; in the more destabilized mutants, Y35G and N43G, there is widespread but variable acceleration of rates. In mutants that are less destabilized than the ones reported here, most buried protons have the same exchange rate constants in WT and mutant (F. Tao, unpublished results).

Relationship of the Slow Exchange Core to the Lumry Knot. Rufus Lumry (1991) has discussed the slowly exchanging protons in proteins and called their locale the knot, part of a knot–matrix model of protein dynamics and function. The knot, as it is envisioned, is far larger than the slow exchange core discussed here; the knot includes the 20–40 slowest exchanging protons, i.e., the number of hydrogens whose rate constants lie within the distribution of slow exchange rates measured by tritium exchange experiments (Lumry, 1991; Lumry & Gregory, 1986; 1989; Gregory & Lumry, 1985). Lumry and Gregory predicted that knots contain the most highly conserved hydrophobic side chains, the atoms of lowest crystallographic *B* factors, and residues of the appropriate hydrophobicity and sequence position necessary to form a single kind of conformation. They suggested that the cooperativity and stability of the knot is enhanced by the confinement of nonpolar groups within and around the hydrogen-bond network, which shrinks the total array to a state of low dielectric constant leading to shortened hydrogen bonds, low motility, and high local density.

Summary. Changes in local flexibility introduced by single site replacements in BPTI have been correlated with changes in structure and folding thermodynamics. Local mobility measured by hydrogen exchange is correlated with local rearrangements of crystal structure around buried mutational sites, suggesting that mutational plasticity and hydrogen exchange reflect the same dynamic property of protein structure. Changes in $\Delta G_{(WT\rightarrow mut)}$ are exceptionally large for these mutants (4.7–6 kcal/mol), and values obtained by hydrogen exchange agree reasonably well with values obtained by calorimetry. There is no correlation of native-state hydrogen exchange rates with stability; the perturbation of internal flexibility by the mutations is highly localized. Comparison of the submolecular region containing the slowest out-exchanging NH to the region containing the NH protected from exchange during folding reveals an important relationship. The most rigid segments of the native structure correspond to the most compact segments in early stages of folding. That is, a property of the native state, local flexibility, identifies the locale of initial events in the folding process.

SUPPLEMENTARY MATERIAL AVAILABLE

Table of NH and $C_\alpha H$ chemical shifts of BPTI mutants discussed in this article (2 pages). Ordering information is given on any current masthead page.

REFERENCES

Baum, J., Dobson, C., Evans, P., & Hanley, C. (1989) *Biochemistry 28*, 7–13.

Buck, M., Radford, S., & Dobson, C. (1993) *Biochemistry 32*, 669–678.

Brown, L., DeMarco, A., Richarz, R., Wagner, G., & Wüthrich, K. (1978) *Eur. J. Biochem. 88*, 87–95.

Carson, M. (1987) *J. Mol. Graphics 5*, 103–106.

Chyan, C.-L., Wormald, C., Dobson, C., Evans, P., & Baum, J. (1993) *Biochemistry* (in press).
Connolly, J. (1983) *Science* 221, 709–713.
Danishefsky, A. T., Housset, D., Kim, K.-S., Tao, F., Fuchs, J., Woodward, C., & Wlodawer, A. (1993) *Protein Sci. 2*, 577–587.
Davis, D. G., & Bax, A. (1985) *J. Am. Chem. Soc. 107*, 2820–2821.
Dill, K. A., Fiebig, K., & Chan, H. S. (1993) *Proc. Natl. Acad. Sci. U.S.A. 90*, 1942–1946.
Edelhoch, H. (1967) *Biochemistry 6*, 1948–1954.
Englander, S. W. (1975) *Ann. N.Y. Acad. Sci. 244*, 10–27.
Englander, S. W., & Englander, J. J. (1978) *Methods Enzymol. XLIX*, 24–39.
Englander, S. W., & Kallenbach, N. R. (1984) *Q. Rev. Biophys. 16*, 521–655.
Fan, P., Bracken, C., & Baum, J. (1993) *Biochemistry 32*, 1573–1582.
Gallagher, W., Tao, F., & Woodward (1992) *Biochemistry 31*, 4673–4680.
Goldenberg, D. P. (1988) *Biochemistry 27*, 2481–2489.
Goodman, E., & Kim, P. (1991) *Biochemistry 30*, 11615–11620.
Green, N. M., & Work, E. (1953) *Biochem. J. 54*, 257–266.
Gregory, R., & Lumry, R. (1985) *Biopolymers 24*, 301–326.
Hilton, B. D., & Woodward, C. K. (1979) *Biochemistry 18*, 5834–5841.
Hilton, B. D., Trudeau, K., & Woodward, C. K. (1981) *Biochemistry 20*, 4697–4703.
Housset, D., Kim, K.-S., Fuchs, J., & Woodward, C. (1991) *J. Mol. Biol. 220*, 757–770.
Hynes, T. R., Randal, M., Kennedy, L. A., Eigenbrot, C., & Kossiakoff, A. A. (1990) *Biochemistry 29*, 10018–10022.
Jackson, W. M., & Brandts, J. F. (1970) *Biochemistry 9*, 2294–2301.
Jeng, M.-F., Englander, S. W., Elöve, G., Wand, A., & Roder, H. (1990) *Biochemistry 29*, 10433–10437.
Kim, K.-S., & Woodward, C. (1993) *Biochemistry 32*, following article in this issue.
Kim, K.-S., Tao, F., Fuchs, J. A., Danishefsky, A. T., Housset, D., Wlodawer, A., & Woodward, C. (1993a) *Protein Sci. 2*, 588–596.
Kim, K.-S., Fuchs, J. A., & Woodward, C. (1993b) Manuscript in preparation.
Kingston, I., & Anderson, S. (1986) *Biochem. J. 233*, 443–450.
Kitaguchi, N., Takahashi, Y., Tokushima, Y., Shiojiri, S., & Ito, H. (1988) *Nature 331*, 530–532.
Levitt, M., & Perutz, M. (1988) *J. Mol. Biol. 201*, 751–754.
Lumry, R. (1991) in *A Study of enzymes, Volume II. Mechanism of Enzyme Action* (Kuby, S. A., Ed.) pp 3–81, CRC Press, Boca Raton, FL.
Lumry, R., & Rosenberg, A. (1975) *Colloq. Int. C.N.R.S. 246*, 53–62.
Lumry, R., & Gregory, R. (1986) in *The Fluctuating Enzyme* (Welch, G. R., Ed.) pp 1–190, Wiley Interscience, New York.
Lumry, R., & Gregory, R. (1989) *J. Mol. Liq. 42*, 113–144.
Marion, D., & Wüthrich, K. (1983) *Biochem. Biophys. Res. Commun. 113*, 967–974.
Miranker, A., Radford, S., Karplus, M., & Dobson, C. (1991) *Nature 349*, 633–636.
Moses, E., & Hinz, H.-J. (1983) *J. Mol. Biol. 170*, 765–776.
Oas, T., & Kim, P. (1988) *Nature 336*, 42–48.
Otting, G., Liepinsh, E., & Wüthrich, K. (1991) *Science 254*, 974–980.
Otting, G., Liepinsh, E., & Wüthrich, K. (1992) *J. Am. Chem. Soc. 114*, 7093–7095.
Pain, R. (1992) *Nature 358*, 278–288.
Pan, Y., & Briggs, M. (1992) *Biochemistry 31*, 11204–11412.
Paterson, Y., Englander, S. W., & Roder, H. (1990) *Science 249*, 755–759.
Pedersen, T., Sigurskjold, B., Andersen, K., Kjaer, M., Poulsen F., Dobson, C., & Redfield, C. (1991) *J. Mol. Biol. 218*, 413–426.
Pedersen, T., Thomsen, N., Andersen, K., Madsen, J., & Poulsen, F. (1993) *J. Mol. Biol. 230*, 651–660.
Ponte, P., Gonzales-DeWhitt, P., Schilling, J., Miller, J., Hsu, D., Greenberg, B., Davis, K., Wallace, W., Lieberburg, I., Fuller, F., & Cordell, B. (1988) *Nature 331*, 525–527.
Privalov, P. L. (1979) *Adv. Protein Chem. 33*, 168–241.
Privalov, P. L., Griko, Y. V., Venyaminov, S. Y., & Kutyshenko, V. P. (1986) *J. Mol. Biol. 190*, 487–498.
Radford, S., Buck, M., Topping, K., Dobson, C., & Evans, P. (1992a) *Proteins: Struct., Funct., Genet. 14*, 237–248.
Radford, S., Dobson, C., & Evans, P. (1992b) *Nature 358*, 302–307.
Richards, F. M. (1979) *Carlesberg Res. Commun. 44*, 47–63.
Richarz, R., Sehr, P., Wagner, G., & Wüthrich, K. (1979) *J. Mol. Biol. 130*, 19–30.
Roder, H., & Wüthrich, K. (1986) *Proteins: Struct. Funct., Genet. 1*, 34–42.
Roder, H., Elöve, G., & Englander, S. W. (1988) *Nature 335*, 700–704.
Sandberg, W. S., & Terwilliger, T. C. (1991) *Proc. Natl. Acad. Sci. U.S.A. 88*, 1706–1710.
Shirley, B. A., Stanssens, P., Hahn, U., & Pace, C. N. (1992) *Biochemistry 31*, 725–732.
Smith, P. K., Krohn, R. I., Hermanson, G. T., Mallia, A. K., Gartner, F. H., Provenzano, M. D., Fujimoto, E. K., Goeke, N. M., Olson, B. J., & Klenk, D. C. (1985) *Anal. Biochem. 150*, 76–85.
Tanzi, R., McClatchey, A., Lamperti, E., Villa-Komaroff, L., Gusella, J., & Neve, R. (1988) *Nature 331*, 528–530.
Tao, F., Fuchs, J., & Woodward, C. (1993) in *Techniques in Protein Chemistry IV* (Angeletti, R., Ed.) pp 549–556, Academic Press, New York.
Tüchsen, E., & Woodward, C. (1985a) *J. Mol. Biol. 185*, 405–419.
Tüchsen, E., & Woodward, C. (1985b) *J. Mol. Biol. 185*, 421–430.
Tüchsen, E., & Woodward, C. (1987a) *J. Mol. Biol. 193*, 793–802.
Tüchsen, E., & Woodward, C. (1987b) *Biochemistry 26*, 1918–1925.
Tüchsen, E., & Woodward, C. (1987c) *Biochemistry 26*, 8073–8078.
Tüchsen, E., Hvidt, A., & Ottesen, M. (1980) *Biochemie 62*, 563–566.
Tüchsen, E., Hayes, J., Ramaprasad, S., Copie, V., & Woodward, C. (1987) *Biochemistry 26*, 5363–5172.
Udgaonkar, J., & Baldwin, R. (1988) *Nature 335*, 694–699.
Wagner, G. (1983) *Q. Rev. Biophys. 16*, 1–57.
Wagner, G., Stassinopoulou, C. I., & Wüthrich, K. (1984) *Eur. J. Biochem. 145*, 431–436.
Wagner, G., Braun, W., Havel, T. F., Schaumann, T., Go, N., & Wüthrich, K. (1987) *J. Mol. Biol. 196*, 611–639.
Well, J. (1990) *Biochemistry 29*, 8509–8517.
Wenzel, H., & Tschesche, H. (1984) *Angew. Chem. 93*, 292–293.
Wlodawer, A., Deisenhofer, J., & Huber, R. (1987a) *J. Mol. Biol. 193*, 145–156.
Wlodawer, A., Nachman, J., Gilliland, G. L., Gallagher, W., & Woodward, C. (1987b) *J. Mol. Biol. 198*, 469–480.
Woodward, C. K., & Rosenberg, A. (1971) *J. Biol. Chem. 246*, 4105–4113.
Woodward, C. K., & Rosenberg, A. (1971) *J. Biol. Chem. 246*, 4114–4121.
Woodward, C. K., & Hilton, B. D. (1980) *Biophys. J. 32*, 561–575.
Woodward, C., Simon, I., & Tüchsen, E. (1982) *Mol. Cell. Biochem. 48*, 135–160.
Wun, T.-C., Kretzmer, K., Girard, T., Miletch, J., & Broze, G. (1988) *J. Biol. Chem. 263*, 6001–6004.